Navier-Stokes equations based Aeroelasticity of Supersonic Transport including Short Period Oscillations

Guru Guruswamy[1]
NASA Ames Research Center, Moffett Field, CA 94035

Nomenclature

C_D = coefficient of total drag

C_L = coefficient of total lift

C_P = coefficient of pressure

d_{SP} = damping of short period oscillation

g = acceleration due to gravity, ft/sec

M = Mach number

q = pitch rate

Q = dynamic pressure in lbs/sqft

S = surface area in sqft

u_0 = initial velocity, ft/sec

V = flight-path velocity vector

α = angle of attack in degrees

ω_{SP} = frequency of short period oscillation in radians/sec

I Introduction

There is renewed interest in developing new supersonic transports [1] after the discontinuation of the Concorde supersonic jet [2], which was mostly limited for flights over trans-oceanic routes due to the severe noise of the sonic boom. In order to avoid the sonic boom, more slender configurations, such as the Low

[1] Sr. Aerospace Engineer, Computational Physics Branch, AIAA Associate Fellow

Boom Flight Demonstrator (LBFD) configuration [3], are being considered. The aeroelastic characteristics of these new supersonic transports can significantly differ from conventional aircraft. Both rigid and flexible body modes can play a significant role in aeroelastic stability. For unconventional configurations, such as aircraft with forward swept wings, the short period oscillation (SPO) has been found to significantly impact the aeroelastic response [4]. SPO can occur due to unanticipated events such as gusts, abrupt maneuvering, etc. During the design of the Concorde, the effects of SPO was considered in detail, though its impact is not publically disclosed [5].

Assuring stability of supersonic aircraft, particularly during descent from the supersonic Mach regime to the transonic regime, is critical. An aircraft can deviate from its normal descent trajectory due to coupling between flows and body motions. The effect of SPO needs to be considered in aeroelastic responses. Preliminary studies using quasi-steady aerodynamics show that the presence of SPO can lead to unstable response [6]. The well-established Reynolds Averaged Navier-Stokes (RANS) equations, which are computationally feasible with current supercomputers, have been in use for aeroelastic computations for the last three decades [7]. Recently, such efforts have begun to include trajectory motions [8]; for instance, the effect of phugoid motion on stability is studied in Ref. 9 using the RANS equations.

In this paper, the effect of SPO on aeroelastic responses of a typical supersonic transport is studied.

I Short Period Oscillation Equations of Motion

Following the derivations of Ref. 10, the frequency of short period oscillations is defined as:

$$\omega_{sp} = \frac{M_q Z_\alpha}{u_0} \tag{1}$$

where $M_q = C_{mq} lQSc/(2u_0 I_y)$, $Z_\alpha = u_0 Z_w$, $Z_w = -QS(\frac{1}{mu_0})(C_{l\alpha} + C_{d0})$, C_{mq} is the pitching moment coefficient with respect to pitch rate (q), l is the reference length (root chord), Q is the dynamic pressure, S is surface area, c is mean aerodynamic chord, u_0 is initial velocity, I_y is moment of inertia about center of gravity, m is mass of aircraft, $C_{l\alpha}$ is lift coefficient, and C_{d0} is initial drag coefficient.

The damping is defined as:

$$d_{sp} = -0.5(\frac{1}{\omega_{sp}})(M_\alpha + M_{\dot{\alpha}} + \frac{Z_\alpha}{u_0}) \qquad (2)$$

where $M_\alpha = u_0 M_w;\ M_{\dot{\alpha}} = u_0 M_{\dot{w}};\ M_w = C_{m\alpha} QSc/u_0 I_y;\ M_{\dot{w}} = C_{m\dot{\alpha}} \frac{c}{2u_0} (QSc/u_0 I_y)$

These equations are superimposed on the aeroelastic equations of motion [11].

$$[W]\{h\} + [G]\{\ddot{h}\} + [\dot{K}]\{h\} = \{F\} \qquad (3)$$

where [W], [G], and [K] are the modal mass, damping, and stiffness matrices, respectively. {F} and {h} are generalized aerodynamic force and displacement vectors, defined as:

$$\{F\} = Q[\psi][A]\{c_p\} \qquad (4)$$

where ψ is the transpose of mode shape matrix, [A] is the control area matrix of the CFD grid, and {c_p} is the average pressure coefficient on the CFD control area. The structural damping G is assumed to be negligible compared to aerodynamic damping. The aerodynamic unsteady load vector {F} is computed by solving the RANS equations.

In this work, Eq. (3) is solved using the Newmark's time integration method in association with the instantaneous Lagrangian-Eulerian approach (also known as Arbitrary-Lagrangian-Eulerian [ALE]) [12], with the aerodynamic data computed by solving the RANS equations [13]. For this work, the RANS equations are numerically solved using the OVERFLOW code [14], which uses the diagonal form of the Beam-Warming central difference algorithm [15], along with the one-equation Spalart-Allmaras turbulence model [16]. An aeroelastic solution module is embedded into the OVERFLOW code and validated with wind tunnel data for a rectangular wing [17]. Figure 1 shows the aeroelastic responses at M_∞ = 0.90. Computed results show neutrally stable response at Q = 1.25 psi compared to 1.20 as measured in the wind tunnel [17].

Starting from the converged steady state solution for a given Mach number, time integration of Eq. (3) is solved with and without superposition of SPO applied while vehicle is experiencing stable aeroelastic oscillation such as limit-cycle oscillation(LCO). SPO simulates induced oscillation due to abrupt gust or sudden changes in maneuvering. The effects of SPO on aeroelastic oscillations are then studied.

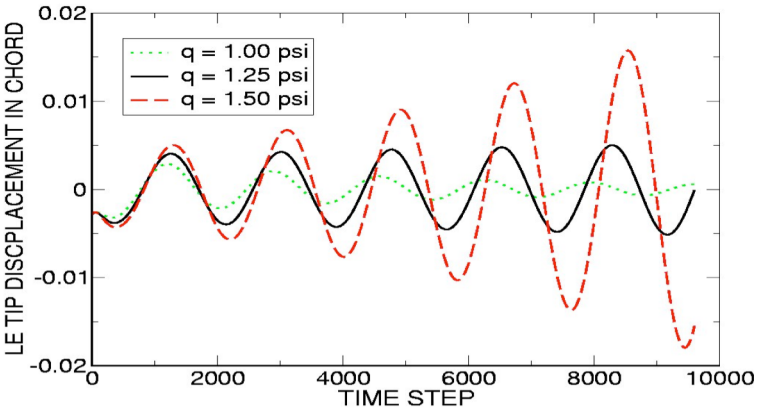

Fig.1. Dynamic aeroelastic responses at M_∞ = 0.90. Measured flutter dynamic pressure q = 1.20 psi, from [17].

II Results

A generic supersonic transport conceived by NASA Langley Research Center [18] was selected for demonstration since it exists in the public domain. A grid that satisfies engineering requirements, such as in spacing and stretching factors, was selected from Ref. 9. Figure 1 shows alternate grid lines of the surface grid including the wake grid (red), defined by 174 points in the axial-direction (x) and 422 points in the circumferential direction (y-z), and near-body section grid at the tail. With H-O topology (H meaning stacked as surfaces in the x-direction and O meaning each surface wrapped around the body), the outer boundary surfaces are placed at a distance of about 15 vehicle lengths using 75 grid points. Numerical experiments similar to that reported in Ref. 9 were performed for this grid to assess its

resolution quality. The selected grid of size 422x174x75 is found adequate to give acceptable force quantities needed for this work.

This grid was validated with wind tunnel data and the linear theory results as reported in Ref. 9. Figure 3 shows typical flow results at M_∞= 0.90.

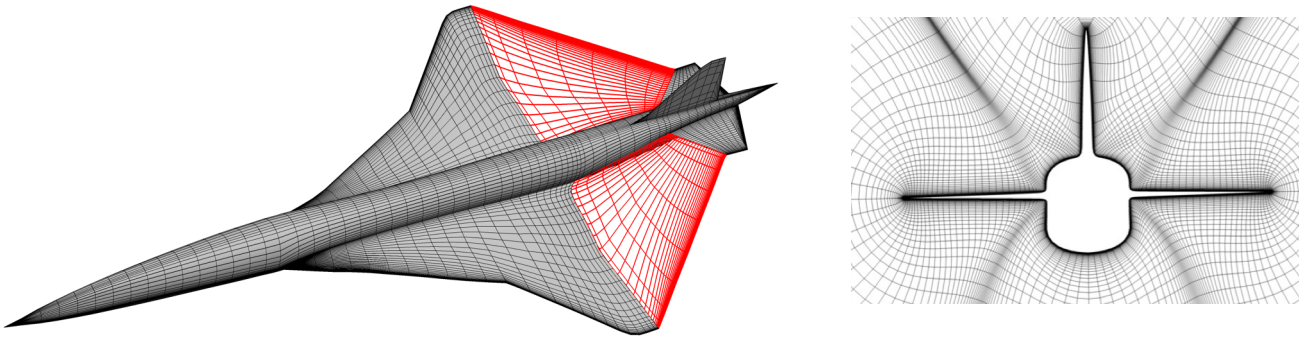

(a)

(b)

Fig. 2. Grids : a) Surface and wake (red) grids of a typical supersonic transport.
b) Section grid at the tail.

.

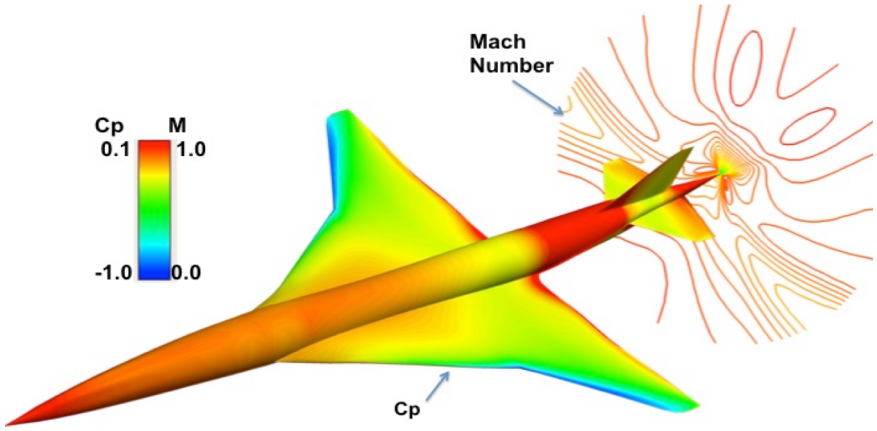

Fig. 3. Surface Cp and tail region Mach number distributions at M_∞ = 0.90, α = 5 degs.

By using the structural properties of a typical supersonic transport [18], Eq. (3) is solved at Mach numbers 0.70 and 0.90 with and without superposition of SPO. Figure 6 shows the first bending and torsion modes of the aircraft obtained using a stick-model [19].

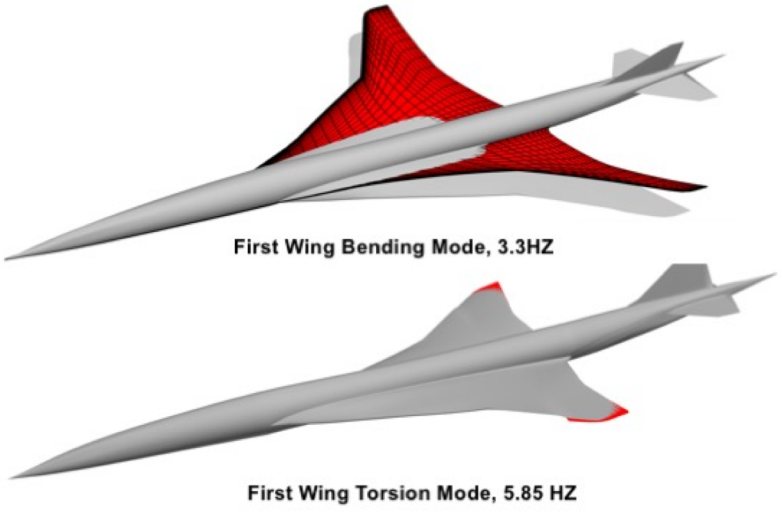

Fig. 4 First two modes and frequencies**.**

Based on Eqns. 1 and 2, the short period oscillatory motion is computed at M_∞= 0.70 and 0.90. Figure 5 shows the damped motion of duration 0.08 seconds for M_∞= 0.90 with assumed initial angle attack of 3 deg.

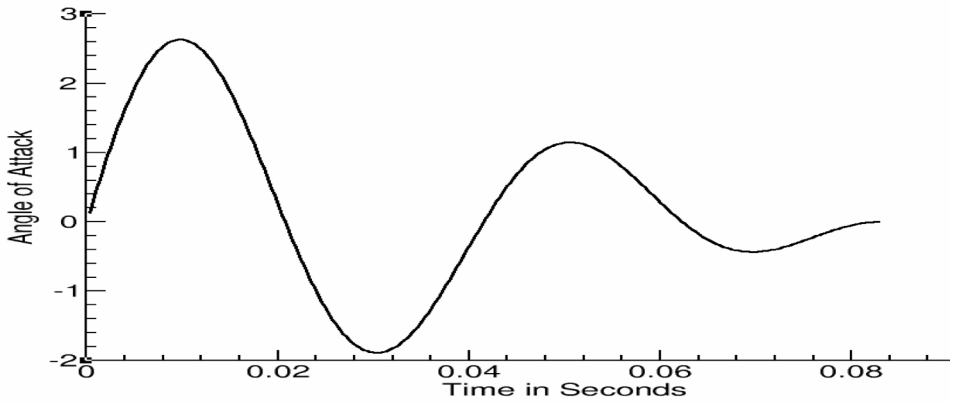

Fig. 5 Short Period Motion at M_∞ = 0.90.

Computations are first made by solving Eq. 3 without SPO. A well-established time integration method [11] is used to solve Eq. 3. It is found that near-limit-cycle oscillations occur at Q = 130 and 80 lbs/sqft at M_∞ = 0.70 and 0.90, respectively. The SPO is superimposed on this response at a time of 0.5 secs. Figure 6 shows responses with and without SPO for M_∞ = 0.70. Without SPO, the limit cycle response is mostly close to the twist mode. With SPO, the response is initially magnified but finally reaches a neutrally stable condition. Figure 7 shows responses of the first generalized displacement with and without SPO for M_∞= 0.90. The response without SPO is neutrally stable with contributions from both bending and torsion modes. The addition of SPO finally leads to a diverging response.

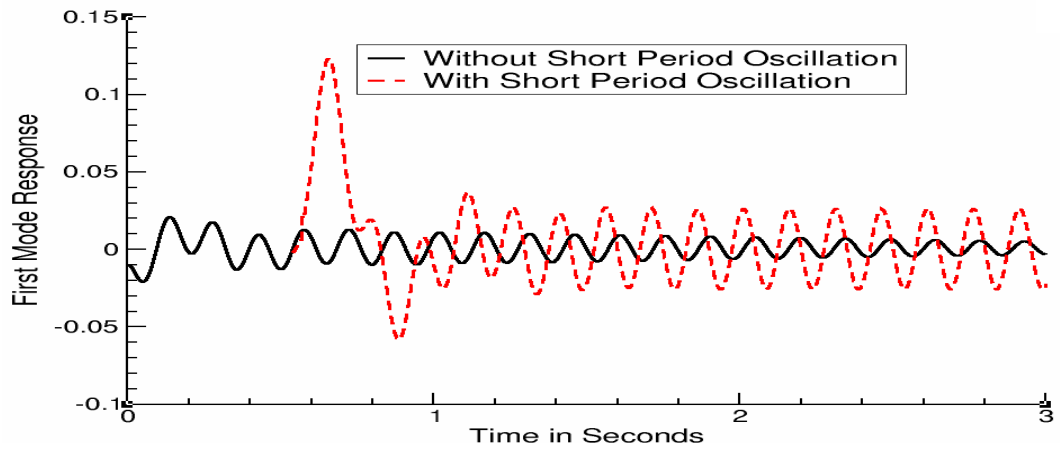

Fig 6. Responses with and without SPO at M_∞ = 0.70

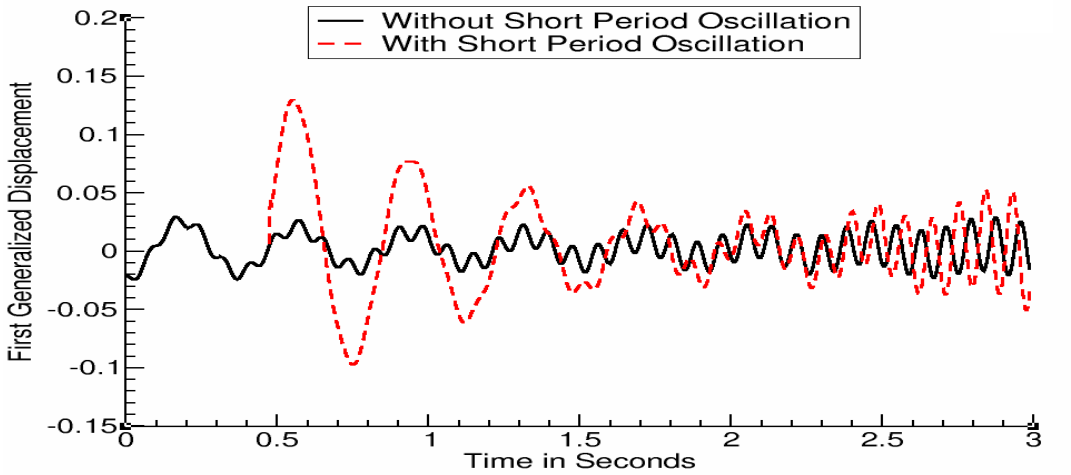

Fig. 7 Responses with and without SPO at M_∞ = 0.90.

III Concluding Remarks

This work presents a complete time-accurate procedure based on the RANS equations to compute responses including short period oscillations (SPO). The procedure presented in this paper will help in the design of highly slender, next-generation supersonic transports. The fully time-accurate approach presented here can be used to determine if aeroelastic oscillations are initiated from short period oscillations. Present computations show that SPO can make a system less stable in the transonic regime. Demonstration of use of the RANS equations for advanced aeroelastic applications as presented in this paper can help to expand the scope of new CFD codes such as FUN3D [20] and LAVA [21] that are under development based on modified RANS algorithms. Future work involves modeling active controls [22] to alleviate aeroelastic instabilities due to SPO.

Acknowledgements

This work was partially supported under applied research activity of the NASA Advanced Supercomputing Division (NAS), Ames Research Center.

References

1) NASA News Release Feb. 16-202, 'NASA Begins Work to Build Quieter Supersonic Passenger jet', February 2016 (https://www.nasa.gov/press-release/nasa-begins-work-to-build-a-quieter-supersonic-passenger-jet, date accessed Oct 30, 2017)

2) Lawless, J. "Final Concorde Flight Lands at Heathrow", Washington Post, October 24, 2003; (http://www.washingtonpost.com/wp-dyn/articles/A11477-2003Oct24.html, Date accessed Oct 30, 2017).

3) Ordaz, I., Geiselhart, K., Fenbert J. W. "Conceptual Design of Low Boom Supersonic Aircraft with Flight Trim Requirement," AIAA 2014-2141, 32nd AIAA Applied Aerodynamics Conference, June 2014.

4) Miller, G. D, Wykes, J. H. and Brosnan, M. J. "Rigid-Body Structural Mode Coupling on a Forward Swept Wing Aircraft," J. of Aircraft, Vol. 20, NO. 8, Aug 1983, pp 696-702.

5) Broadbent, E. G., Zbrozek, J. K., and Huntley, E., "A Study of Dynamic Aeroelastic Effects on the Stability Control and Gust Response of a Slender Delta Aircraft," R&M No 3690, Aeronautical Research Council, UK 1972.

6) Baldelli D. H., Chen, P.C and Panza, J., "Unified Aeroelastic and Flight Dynamic Formulation via Rational Function Approximations," J. of Aircraft, Vol. 43, No. 3, May–June 2006, pp. 763-772.

7) Guruswamy, G.P., "Computational Aeroelasticity," Part 3, Sections 3.45-3.50, The Standard Handbook for Aerospace Engineers, McGraw-Hill, Feb. 2018, pp. 273-285.

8) Guruswamy, G. P., "Time Accurate Coupling of 3-DOF Parachute System with Navier-Stokes Equations," J. of Spacecraft and Rockets, Vol. 54, No. 6, November–December 2017, pp.1278-1283.

9) Guruswamy, G. P., "Phugoid Motion Simulation of a Supersonic Transport using Navier-Stokes Equations," (to appear in AIAA journal).

10) Nelson, C. R., "Flight Stability and Automatic Control" Section 4.5, 2nd Edition WCB/McGraw-Hill, ISBN-13: 978-0070462731,1998.

11) Guruswamy, G.P., "Computational-Fluid-Dynamics and Computational-Structural-Dynamics Based Time-Accurate Aeroelasticity of Helicopter Blades," J. of Aircraft, Vol. 47, No. 3, May-June 2010, pp. 858-863.

12) Guruswamy, G. P, "Time-Accurate Aeroelastic Computations of a Full Helicopter Model using the Navier-Stokes Equations," International J. of Aerospace Innovations, Vol. 5, No 3+4, Dec 2013, pp. 73-82.

13) Peyret, R., and Viviand, H., "Computation of Viscous Compressible Flows Based on Navier–Stokes Equations," AGARD AG-212, 1975.

14) Nichols, R. H., Tramel R.W., and Buning P.G., "Solver and Turbulence Model Upgrades to OVERFLOW2 for Unsteady and High-Speed Applications," AIAA Paper 2006-2824, AIAA 36th Fluid Dynamics Conference, San Francisco, CA, June 2006.

15) Beam, R. M., and Warming, R. F., "An Implicit Factored Scheme for the Compressible Navier–Stokes Equations," AIAA Journal, Vol. 16, No. 4, 1978, pp. 393–402.

16) Spalart, P. R., and Allmaras, S., "A One-Equation Turbulence Model for Aerodynamic Flows," AIAA Paper 92-0439, Aerospace Sciences Meeting, Reno, NV, 1992.

17) Dogget, R.V., Rainey, A.G, and Morgan, H.G., "An Experimental Investigation on Transonic Flutter Characteristics," NASA TMX-79, Nov. 1959.

18) Raney, D. L., Jackson, E. B., and Buttrill, C.S., "Simulation Studies of Impact of Aeroelastic Characteristics on Flying Qualities of a high Speed Civil Transport," NASA TP 2002-211943, Oct 2002.

19) Guruswamy, G. P., "Coupled Finite-Difference/Finite-Element Approach for Wing-Body Aeroelasticity," AIAA 92-4680, 4th AIAA/USAF/NASA/OAI Symposium on Multidisciplinary Analysis and Optimization, September, 1992, Cleveland, Ohio.

20) Chawalowski, P. Heeg, J. "FUN3D Analyses in Support of the Second Aeroelastic Prediction Workshop," AIAA 2016-3122, 34th AIAA Applied Aerodynamics Conference, 2016.

21) Kiris, C. C., Barad, M. F., Housman, J. A., Sozer, E., Brehm, C. and Moini-Yekta, S. "The LAVA Computational Fluid Dynamics Solver," AIAA 2014-0070, 52nd Aerospace Sciences Meeting, Jan. 2014.

22) Guruswamy, G. P., "Integrated Approach for Active Coupling of Structures and Fluids", AIAA Jl., Vol. 27, No. 6, June 89, pp. 788-793